Effect of the Amorphous Segment on the Nonisothermal Crystallization and Morphology of Oxyethylene–Oxybutylene Block Copolymers

Jun-Ting Xu,[1] Liang Xue,[1] Shao-Min Mai,[2] A. J. Ryan[2]

[1]*Department of Polymer Science and Engineering, Zhejiang University, Hangzhou 310027, China*
[2]*Chemistry Department, University of Sheffield, Sheffield S3 7HF, United Kingdom*

Received 5 June 2003; accepted 2 February 2004
DOI 10.1002/app.20490
Published online in Wiley InterScience (www.interscience.wiley.com).

ABSTRACT: The nonisothermal crystallization and morphology of three oxyethylene–oxybutylene block copolymers with different architectures ($E_{50}B_{70}$, $B_{65}E_{75}B_{65}$, and $E_{35}B_{114}E_{35}$) were compared with those of three blends ($E_{56}B_{27}/B_{14}$, $B_{37}E_{77}B_{37}/B_{14}$, and $E_{38}B_{38}E_{38}/B_{14}$) with the same composition and morphology (E and B represent oxyethylene and oxybutylene units, respectively, and the subscripts denote the degree of polymerization), and the effect of the amorphous block was examined. The neat block copolymers had larger *d*-spacings and higher melting temperatures than the corresponding blends. In nonisothermal crystallization, the neat block copolymers had lower crystallization temperatures at high cooling rates. The difference in the crystallization temperatures became smaller at low cooling rates, and some of the neat block copolymers could have higher crystallization temperatures. Polarized optical microscopy showed that the neat block copolymers had smaller dimensions of crystal growth and smaller size of spherulites than the blends. The lower crystallization temperatures and less perfect morphology were attributed to the slower rate of conformational rearrangement of the amorphous block, which was required by the chain folding of the crystallizable block. This effect was more evident in the $E_{35}B_{114}E_{35}$ triblock copolymer, in which both ends of the amorphous B block were immobilized at the interface. © 2004 Wiley Periodicals, Inc. J Appl Polym Sci 93: 870–876, 2004

Key words: blends; block copolymers; crystallization; morphology

INTRODUCTION

In semicrystalline block copolymers, crystallization not only depends on the crystallizable block but also is greatly influenced by the amorphous block because the blocks, having different properties, are chemically linked and a microphase-separated morphology is formed. First, chain folding of the crystallizable block is affected by the amorphous block. The amorphous block tends to adopt a random coil conformation, which requires a larger interface area and thus larger chain folds of the crystallizable block. However, an extended chain conformation is most stable for the crystallizable block and leads to a smaller interface area and larger deformation of the amorphous block. The final conformation of the semicrystalline block copolymer is determined by the balance of the crystallizable block and the amorphous block.[1,2] As a result, the crystallizable block adopts a chain-folded conformation, and there is deformation to some extent for the amorphous block as well.[3] Moreover, the crystallization mechanism and morphology after the crystallization of the block copolymer may be different from those of the corresponding homopolymer. Some particular phenomena have been observed in the crystallization of block copolymers. For example, crystallization can occur in confined nanoscale domains,[4–6] and crystallization can be initiated by heterogeneous nucleation, homogeneous nucleation, or mixed mechanisms.[7–9]

To account for the effect of the amorphous block, the crystallization behavior and morphology of semicrystalline block copolymers are usually compared with those of homopolymers or blends.[10] However, microphase separation is a unique morphology in block copolymers and cannot be obtained in homopolymers or blends. As a result, both the amorphous block and microphase-separated morphology affect the crystallization of block copolymers. It is difficult to distinguish these two effects. In this work, we used oxyethylene–oxybutylene block copolymers containing shorter amorphous oxybutylene blocks for blending with the amorphous oxybutylene homopolymer. The crystallization behavior and morphology of

Correspondence to: J.-T. Xu (xujt@zju.edu.cn).
Contract grant sponsor: National Natural Science Foundation of China (NSFC); contract grant number: 20374046.
Contract grant sponsor: The Excellent Young Teachers Program of the Ministry of Education, China (EYTP).

© 2004 Wiley Periodicals, Inc.

the blends were compared with those of neat block copolymers having crystallizable blocks of similar length and the same composition. Because both the blends and the neat block copolymers were microphase-separated and had the same morphology, the effect of the morphology could be ignored, and the effect of the amorphous block on the crystallization of block copolymers could be examined well.

EXPERIMENTAL

Materials

The synthesis, characterization, and properties of oxyethylene–oxybutylene copolymers with various architectures ($E_{56}B_{27}$, $E_{50}B_{70}$, $B_{37}E_{77}B_{37}$, $B_{65}E_{75}B_{65}$, $E_{38}B_{38}E_{38}$, and $E_{35}B_{114}E_{35}$, where E and B represent oxyethylene and oxybutylene units, respectively, and the subscripts denote the degree of polymerization), have been described elsewhere.[11] These block copolymers had narrow molecular weight distributions. The other poly(oxybutylene) (PBO) homopolymer, with a number-average molecular weight of 1000 (B_{14}), was specially synthesized by anionic polymerization with a narrow molecular weight distribution.

Preparation of the blends

$E_{56}B_{27}$, $B_{37}E_{77}B_{37}$, and $E_{38}B_{38}E_{38}$ were used to blend with B_{14}. The volume fractions of the E block in the blends were set the same as in $E_{50}B_{70}$ (ϕ_E = 0.270), $B_{65}E_{75}B_{65}$ (ϕ_E = 0.237), and $E_{35}B_{114}E_{35}$ (ϕ_E = 0.245), respectively. The blends of the block copolymers with PBO were prepared by a solution-blending method with dicholoromethane as a solvent. To ensure that the PBO homopolymer was miscible with the PBO segments in the block copolymers and that the condition of the wet brush was met, the molecular weight of the PBO homopolymer was half that of the PBO block.[12,13] The blends were dried *in vacuo* for 24 h at 60°C after the solvent was evaporated, and then they were cooled to room temperature slowly and stored below 0°C until they were used.

Nonisothermal crystallization

The nonisothermal crystallization of the pure block copolymers and blends was performed on a PerkinElmer Pyris-1 calorimeter (Boston, MA). Samples sealed in aluminum pans were heated to 70°C, held for 5 min, and then cooled at a prescribed cooling rate until the crystallization was completed. The thermal lag was ignored and not corrected.

Small-angle X-ray scattering (SAXS)

The SAXS experiments were carried out for the crystallized samples at room temperature on Beam Line 8.2 of the Synchrontron Radiation Facility (SRS, Daresbury, UK). The samples were held at 70°C for 5 min and then cooled to crystallize at a rate of 10°C/min. Details of the instrument and data processing are described elsewhere.[14,15]

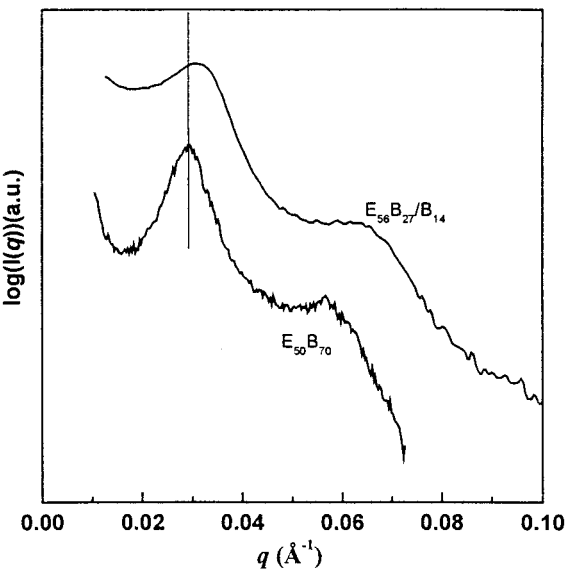

Figure 1 SAXS profiles of $E_{56}B_{27}/B_{14}$ and $E_{50}B_{70}$ after crystallization.

Polarized optical microscopy

Polarized optical microscopy experiments were conducted on an Olympus BX50 microscope (Tokyo, Japan) connected to a Panasonic NV-HD660 video recorder (Osaka, Japan). Samples approximately 1 μm thick were heated to 70°C and held for 5 min with a Linkam hot stage equipped with a liquid N_2 cooling system (Surrey, UK). Afterward, the samples were cooled at a rate of 5°C/min, and the texture of the samples during crystallization was recorded.

RESULTS AND DISCUSSION

d-Spacing

The SAXS patterns of the neat block copolymers and the blends after crystallization from the melts at a rate of 10°C/min are shown in Figures 1–3. A lamellar morphology was formed for all the samples after crystallization despite the cylinder morphology in the melt. The SAXS higher order peaks were not obvious in $E_{38}B_{38}E_{38}/B_{14}$ and $E_{35}B_{114}E_{35}$ because of the slightly broad molecular weight distribution, but after shearing they became evident (this is not shown here). Another common feature in Figures 1–3 is that the neat block copolymers had larger *d*-spacings and thus larger lamellar thicknesses of the E crystals than the corresponding blends, although the neat block copol-

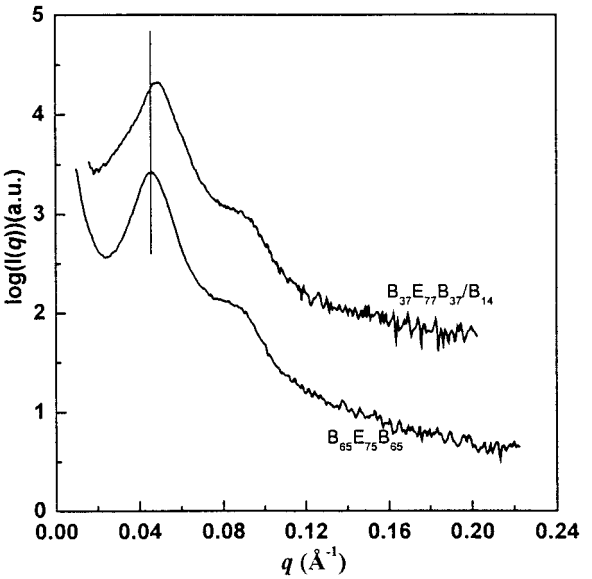

Figure 2 SAXS profiles of $B_{37}E_{77}B_{37}/B_{14}$ and $B_{65}E_{75}B_{65}$ after crystallization.

ymers and the blends had the same composition. Because all the E blocks in the blends were slightly longer than those in the neat block copolymers, such a difference would have been larger if the E blocks in the blends and the neat block copolymers had the same length. In the semicrystalline block copolymers, chain folding of the crystallizable block was determined by the balance of the conformation entropy of the amorphous block, the fusion enthalpy of the crystalline block, and the interfacial free energy.[16] In the blends, parts of the amorphous component were not connected to the E block and thus had a larger number of conformation; this led to a larger contribution to the total free energy. As a result, the amorphous block underwent less deformation in the blends, and this resulted in a smaller thickness of the amorphous and crystalline layers.

Nonisothermal and melting behavior

Figure 4 shows the differential scanning calorimetry (DSC) traces of $E_{56}B_{27}/B_{14}$ and $E_{50}B_{70}$ cooled at various rates. Two crystallization peaks can be observed for the $E_{56}B_{27}/B_{14}$ blend. With an increasing cooling rate, the crystallization peak at higher temperatures became larger. At a cooling rate of 2°C/min, the crystallization peak at higher temperatures was very small. As expected, the crystallization temperature decreased as the cooling rate increased. In contrast, only a single crystallization peak appeared in $E_{50}B_{70}$. Comparing the crystallization temperatures of these two samples, we can see that $E_{50}B_{70}$ had a lower crystallization temperature at a higher cooling rate (10°C/min), but at cooling rates of 2 and 5°C/min, the crystallization peak of $E_{50}B_{70}$ appeared at higher temperatures than the major peak of the $E_{56}B_{27}/B_{14}$ blend.

The nonisothermal crystallization curves of $B_{37}E_{77}B_{37}/B_{14}$ and $B_{65}E_{75}B_{65}$ are illustrated in Figure 5(a,b), respectively. The $B_{37}E_{77}B_{37}/B_{14}$ exhibited single crystallization at a cooling rate of 2°C/min, and the crystallization became broader at the cooling rate of 5°C/min; then, double crystallization peaks appeared at very low temperatures, which may have fallen into the temperature range of homogeneous crystallization. Figure 5(b) shows that $B_{65}E_{75}B_{65}$ had broad crystallization at a cooling rate of 2°C/min, double crystallization peaks at a cooling rate of 5°C/min, and single narrow peaks at a cooling rate of 10°C/min. The crystallization temperatures of the major peak at cooling rates of 5 and 10°C/min were also far below the normal. Comparing the crystallization temperatures of $B_{37}E_{77}B_{37}/B_{14}$ and $B_{65}E_{75}B_{65}$, we can see that $B_{65}E_{75}B_{65}$ had a lower crystallization temperature than the blend at 5 and 10°C/min, but it exhibited a slightly higher crystallization temperature at 2°C/min.

Figure 6(a) shows the nonisothermal crystallization curves of $E_{38}B_{38}E_{38}/B_{14}$. A single crystallization peak can be observed at all the cooling rates studied. Comparatively, double crystallization peaks—one at a very low temperature—can be observed for $E_{35}B_{114}E_{35}$ at cooling rates of 5 and 10°C/min [Fig. 6(b)]. Moreover, $E_{35}B_{114}E_{35}$ had a lower crystallization temperature than the $E_{38}B_{38}E_{38}/B_{14}$ blend at all the cooling rates studied, but the difference became smaller as the cooling rate decreased.

When comparing the nonisothermal crystallization behavior of the neat block copolymers and the corre-

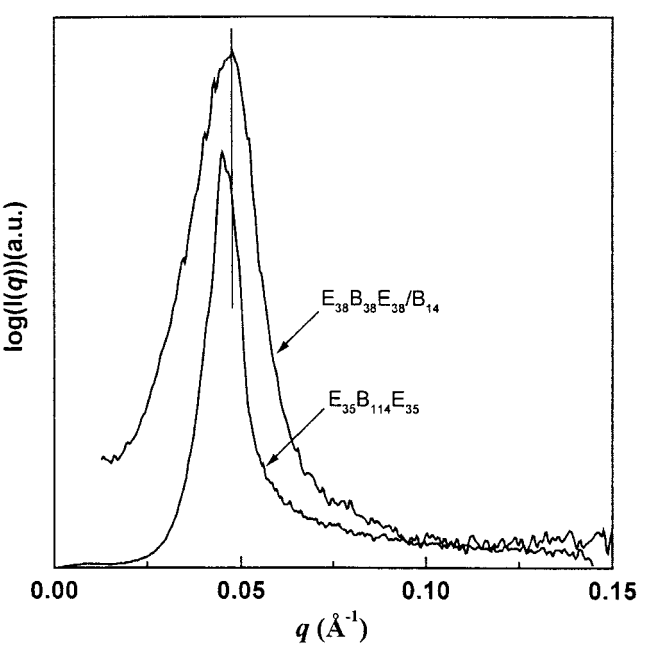

Figure 3 SAXS profiles of $E_{38}B_{38}E_{38}/B_{14}$ and $E_{35}B_{114}E_{35}$ after crystallization.

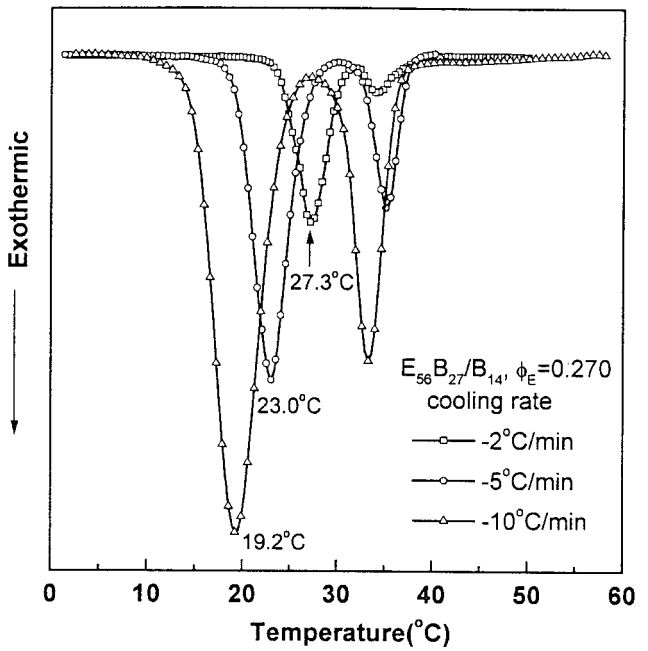

(a)

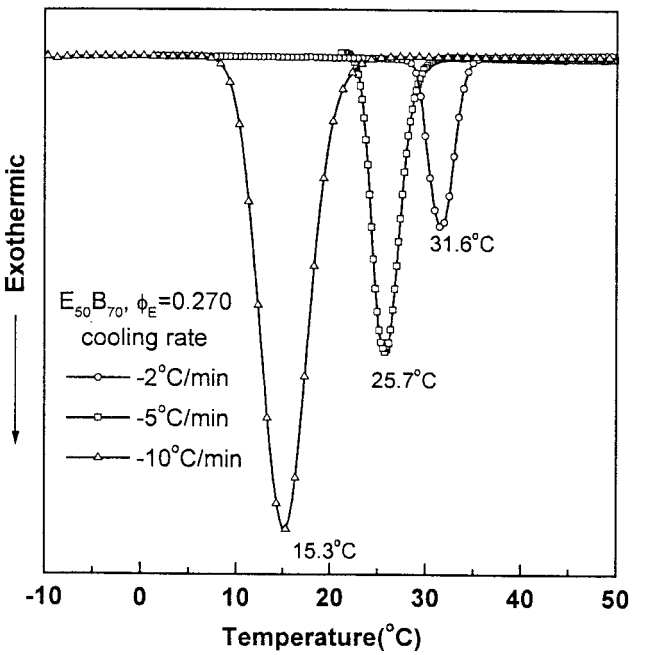

(b)

Figure 4 Nonisothermal crystallization DSC traces of (a) $E_{56}B_{27}/B_{14}$ and (b) $E_{50}B_{70}$ at various cooling rates.

sponding blends, we can see that homogeneous nucleation tended to be more likely to occur for the neat block copolymers, and the crystallization temperature of the neat block copolymers was more easily affected by the cooling rate.

The melting temperatures for the neat block copolymers and the blends at various cooling rates are listed in Table I. The neat block copolymers always exhibited higher melting temperatures than the corresponding blends, and this agreed with the results of SAXS. Because the melting temperature and crystallization temperature of a polymer are related, a polymer with a higher melting temperature usually has a higher crystallization temperature. As shown in Figures 4 and 5, the neat block copolymers $E_{50}B_{70}$ and

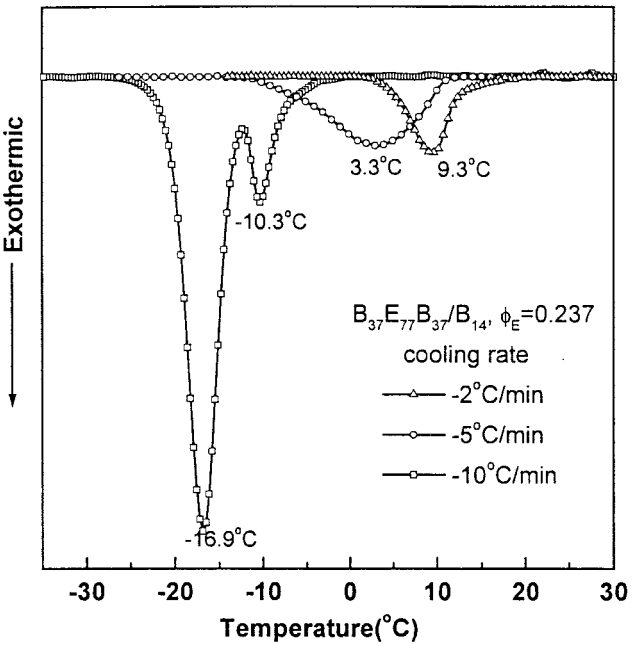

(a)

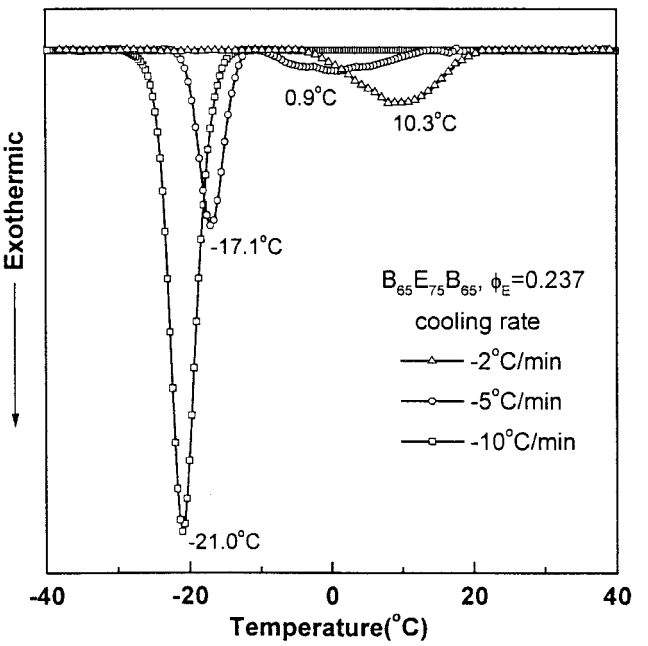

(b)

Figure 5 Nonisothermal crystallization DSC traces of (a) $B_{37}E_{77}B_{37}/B_{14}$ and (b) $B_{65}E_{75}B_{65}$ at various cooling rates.

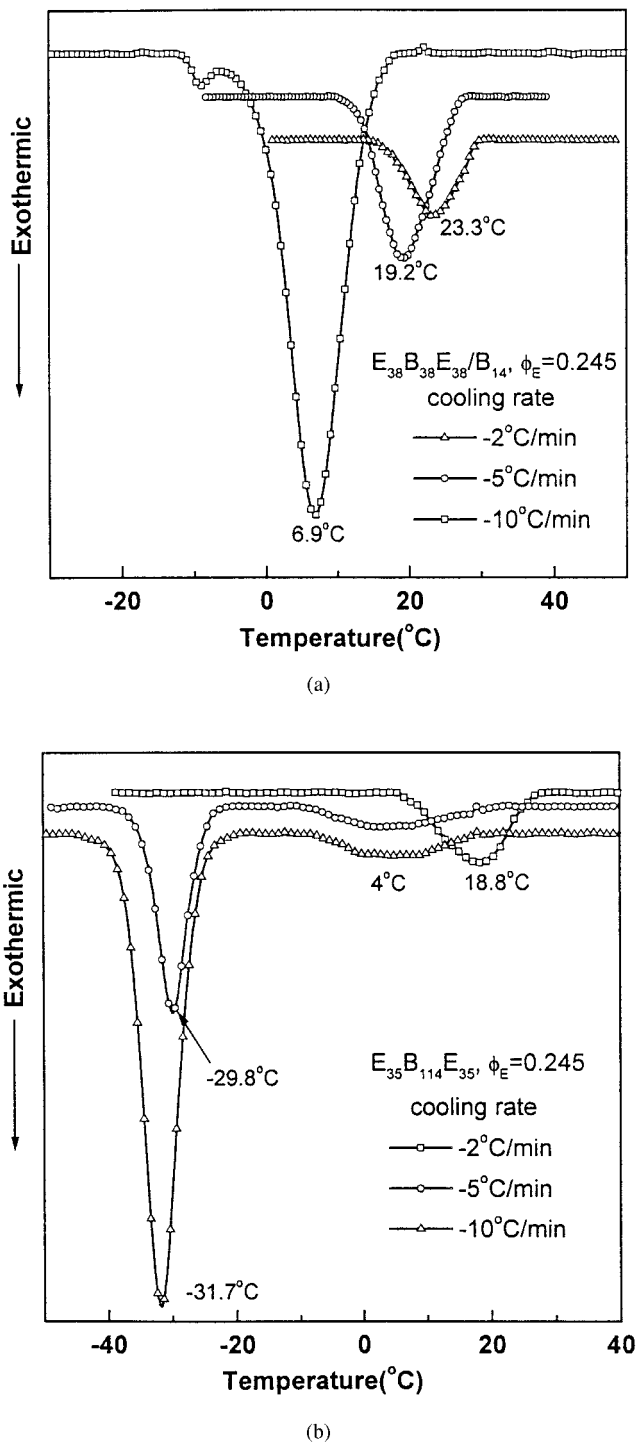

Figure 6 Nonisothermal crystallization DSC traces of (a) $E_{38}B_{38}E_{38}/B_{14}$ and (b) $E_{35}B_{114}E_{35}$ at various cooling rates.

$B_{65}E_{75}B_{65}$ had higher crystallization temperatures than the corresponding blends $E_{56}B_{27}/B_{14}$ and $B_{37}E_{77}B_{37}/B_{14}$ at the cooling rate of 2°C/min. We believe that the lower crystallization temperatures of the neat block copolymers at higher cooling rates arose from the connected longer amorphous block. Chain folding of the crystallizable segment in the block copolymers also led to the deformation of the amorphous block to some extent, which required the conformational rearrangement of the amorphous block during crystallization. In the neat block copolymers, all the amorphous segments were connected to the crystallizable block and had a slower rate of adjusting conformation than those in the blends containing some nonconnected amorphous segments. At a higher cooling rate, the slower conformational rearrangement of the amorphous block retarded crystallization of the E block, and this led to a lower crystallization temperature, whereas there was enough time for the amorphous block to adjust its conformation at a slower cooling rate, and thus the amorphous block had little effect on the crystallization temperature.

The block copolymer $E_{35}B_{114}E_{35}$ also exhibited a lower crystallization temperature than the $E_{38}B_{38}E_{38}/B_{14}$ blend at a cooling rate of 2°C/min, but we could expect $E_{35}B_{114}E_{35}$ to have a higher crystallization temperature at an extremely slow cooling rate because the difference in the crystallization temperatures of $E_{35}B_{114}E_{35}$ and $E_{38}B_{38}E_{38}/B_{14}$ became smaller and smaller as the cooling rate decreased. This also shows that the amorphous B block had a more important influence on the crystallization of the E block in the EBE triblock copolymer than in the EB diblock and BEB triblock copolymers. In our previous work,[17] we compared the crystallization behavior of two triblock copolymers, $E_{91}B_{56}E_{91}$ and $B_{28}E_{182}B_{28}$, which had exactly the same composition and morphology. These two block copolymers had the same *d*-spacing and

TABLE I
Crystallization Temperature and Melting (T_c) Temperature (T_m) of the Neat Block Copolymers and the Blends

Sample	Cooling rate (°C/min)	T_c (°C)	T_m (°C)
$E_{50}B_{70}/B_{14}$	−2	27.3 (m)[a]/33.9	42.8
(ϕ_E = 0.270)	−5	23.0 (m)/35.1	42.8
	−10	19.2 (m)/33.3	42.8
$E_{56}B_{27}$	−2	31.6	44.5
(ϕ_E = 0.270)	−5	25.7	44.0
	−10	15.3	43.1
$B_{37}E_{77}B_{37}/B_{14}$	−2	9.3	35.8
(ϕ_E = 0.237)	−5	3.3	35.8
	−10	−16.9 (m)/−10.3	35.5
$B_{65}E_{75}B_{65}$	−2	10.3	42.1
(ϕ_E = 0.237)	−5	−17.1 (m)/0.9	42.1
	−10	−21.0	41.7
$E_{38}B_{38}E_{38}/B_{14}$	−2	23.3	40.5
(ϕ_E = 0.245)	−5	19.2	40.5
	−10	−9.3/6.9 (m)	35.5
$E_{35}B_{114}E_{35}$	−2	18.8	45.3
(ϕ_E = 0.245)	−5	−29.8 (m)/4.0	44.6
	−10	−31.7 (m)/4.0	44.2

[a] The major crystallization peak.

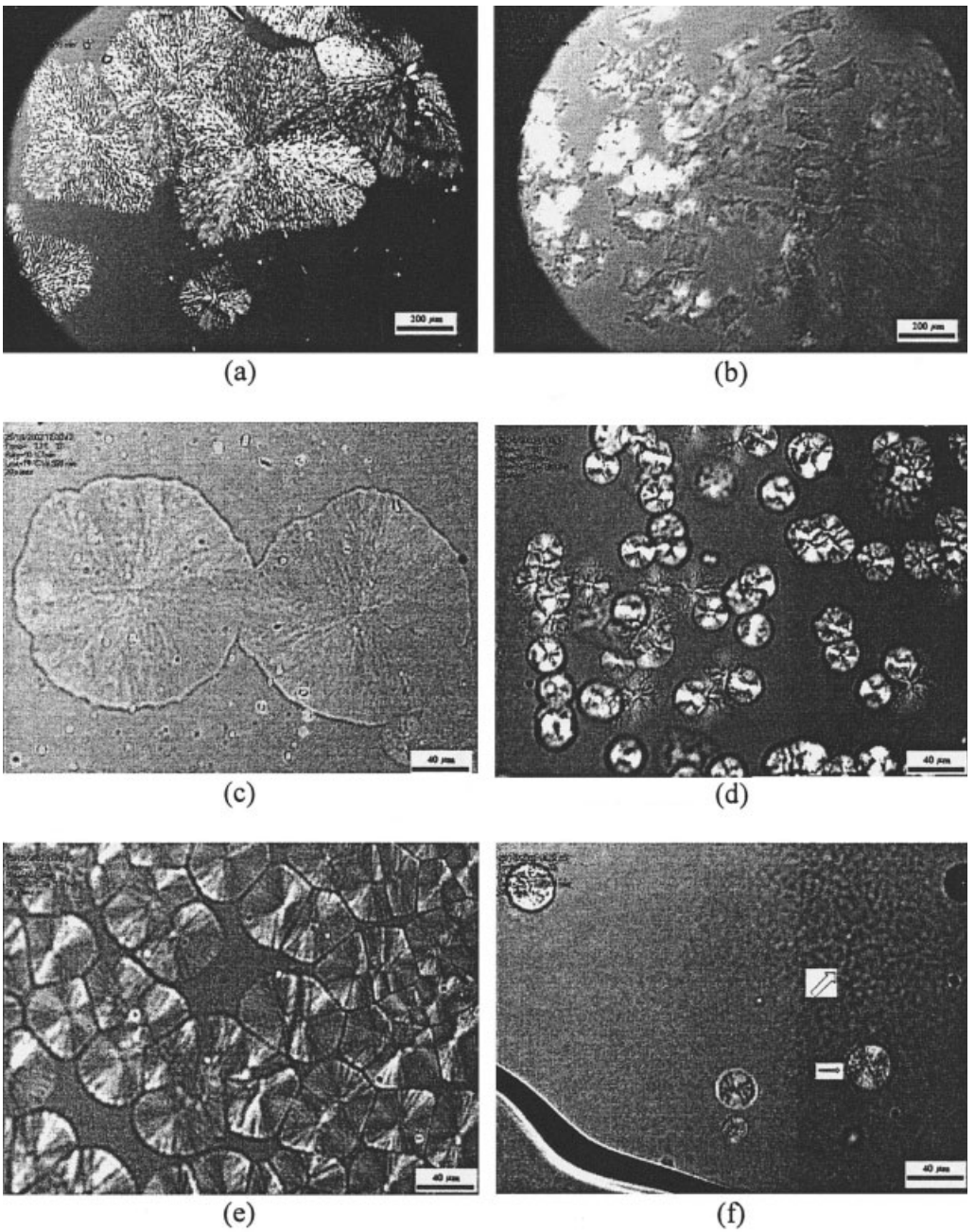

Figure 7 Polarized optical micrographs of (a) $E_{56}B_{27}/B_{14}$, (b) $E_{50}B_{70}$, (c) $B_{37}E_{77}B_{37}/B_{14}$, (d) $B_{65}E_{75}B_{65}$, (e) $E_{38}B_{38}E_{38}/B_{14}$, and (f) $E_{35}B_{114}E_{35}$ during nonisothermal crystallization.

melting temperature, but $E_{91}B_{56}E_{91}$ had a lower crystallization temperature in nonisothermal crystallization and a slower crystallization rate in isothermal crystallization. We speculate that in the EBE triblock copolymer, both ends of the amorphous B block were immobilized at the interface, and it was difficult for the B block to proceed with conformational rearrangement during crystallization.

Polarized optical microscopy

Polarized optical micrographs of the block copolymers and blends are shown in Figure 7. Figure 7(a) reveals that spherulites of large dimensions (ca. 300 μm) with Maltese crosses were formed in $E_{56}B_{27}/B_{14}$, and there were lots of branches inside the spherulites. In contrast, plate crystals instead of spherulites were observed in the neat block copolymer $E_{50}B_{70}$. In $B_{37}E_{77}B_{37}/B_{14}$, the spherulites were approximately 100 μm with no evident Maltese crosses. The neat block copolymer $B_{65}E_{75}B_{65}$ showed spherulite morphology with obvious Maltese crosses, but the dimensions of the spherulites were smaller, about 20–30 μm. Well-defined spherulites were also observed in $E_{38}B_{38}E_{38}/B_{14}$, but $E_{35}B_{114}E_{35}$ showed double models of morphol-

ogy. Some spherulites were observed, and nonspherulite domains appeared as well [both are indicated by arrows in Fig. 7(f)]. The spherulites and nonspherulite domains may have been produced by heterogeneous nucleation and homogeneous nucleation, respectively. Comparing the macroscopic morphology of the neat block copolymers and the corresponding blends, we can see that the neat block copolymers had smaller dimensions of crystal growth and smaller spherulites. This can also be attributed to the low mobility caused by the connected amorphous block.

CONCLUSIONS

The neat block copolymers had larger *d*-spacings and higher melting temperatures than the corresponding blends because the amorphous segments made greater contributions to the total free energy, and this led to larger chain folds of the crystallizable block. However, the neat block copolymers exhibited lower crystallization temperatures at high cooling rates because the connection between the two blocks reduced the rate of conformational rearrangement of the amorphous block; this was required by the chain folding of the crystallizable block. Polarized optical microscopy showed that the neat block copolymers had comparatively less perfect morphology than the blends, such as smaller dimensions of crystal growth and smaller spherulites.

C. Booth of the University of Manchester is acknowledged for providing the block copolymers.

References

1. DiMarzio, E. A.; Guttman, C. M.; Hoffmann, J. D. Macromolecules 1980, 13, 1194.
2. Whitmore, M. D.; Noolandi, J. Makromol Chem Macromol Symp 1988, 16, 235.
3. Ryan, A. J.; Fairclough, J. P. A.; Hamley, I. W.; Mai, S. M.; Booth, C. Macromolecules 1997, 30, 1723.
4. Loo, Y. L.; Register, R. A.; Ryan, A. J. Phys Rev Lett 2000, 84, 4120.
5. Loo, Y. L.; Register, R. A.; Ryan, A. J. Macromolecules 2002, 35, 2365.
6. Xu, J. T.; Fairclough, J. P. A.; Mai, S. M.; Ryan, A. J.; Chaibundit, C. Macromolecules 2002, 35, 6937.
7. Chen, H. L.; Hsiao, S. C.; Lin, T. L.; Yamauchi, K.; Hasegawa, H.; Hashimoto, T. Macromolecules 2001, 34, 671.
8. Xu, J. T.; Turner, S. C.; Fairclough, J. P. A.; Mai, S. M.; Ryan, A. J.; Chaibundit, C.; Booth, C. Macromolecules 2002, 35, 3614.
9. Muller, A. J.; Balsamo, V.; Arnal, M. L.; Jakob, T.; Schmalz, H.; Abetz, V. Macromolecules 2002, 35, 3048.
10. Unger, R.; Reuter, H.; Horing, S.; Donth, E. Polym Plast Technol Eng 1990, 29, 1.
11. Ryan, A. J.; Mai, S. M.; Fairclough, J. P. A.; Hamley, I. W.; Booth, C. Phys Chem Chem Phys 2001, 3, 2961.
12. Tanaka, H.; Hasegawa, H.; Hashimoto, T. Macromolecules 1991, 24, 240.
13. Winey, K. I.; Thomas, E. L.; Fetters, L. J. Macromolecules 1992, 25, 2645.
14. Chaibundit, C.; Mingvanish, W.; Turner, S. C.; Mai, S. M.; Fairclough, J. P. A.; Ryan, A. J.; Matsen, M. W.; Booth, C. Macromol Rapid Commun 2000, 21, 964.
15. Mai, S. M.; Mingvanish, W.; Turner, S. C.; Chaibundit, C.; Fairclough, J. P. A.; Heatley, F.; Matsen, M. W.; Ryan, A. J.; Booth, C. Macromolecules 2000, 33, 5124.
16. Whitmore, M. D.; Noolandi, J. Macromolecules 1988, 21, 1482.
17. Xu, J. T.; Liang, G. D.; Fan, Z. Q. Polym J, accepted.